Biomass Conversion and Biorefinery (2025) 15:8809–8819
https://doi.org/10.1007/s13399-024-05539-9

ORIGINAL ARTICLE

Influential biosorption of lead ions from aqueous solution using sand leek (*Allium scorodoprasum* L.) biomass: kinetic and isotherm study

Zeynep Mine Şenol[1] · **Hasan Arslanoğlu**[2]

Received: 7 February 2024 / Revised: 13 March 2024 / Accepted: 20 March 2024 / Published online: 26 March 2024
© The Author(s) 2024

Abstract
In this study, a zero-cost, naturally effective adsorbent, sand leek (*Allium scorodoprasum* L.), was used for the effective removal of lead ions from an aqueous solution. This natural adsorbent was characterized by FT-IR, SEM–EDX, and PZC analyses. Batch studies were conducted at one factor at a time to explore maximum removal efficiency in terms of pH, initial lead(II) ion concentration, contact time, adsorbent dosage, and temperature for efficient adsorption. The maximum lead(II) ion uptake capacity for SAC was obtained at pH 4.5, initial lead(II) ion concentration at 1000 mg/L, operation time of 1440 min, adsorbent dosage of 10 g, and temperature of 25 °C. The adsorption data were well-fitted by the Freundlich isotherm model, with an R^2 value of 1.000, indicating a good fit. The kinetic study revealed that the adsorption of lead(II) ions followed a pseudo-first-order kinetic model, with an R^2 value of 0.9746. Furthermore, the thermodynamic parameters including Gibbs-free energy change ($\Delta G°$), enthalpy change ($\Delta H°$), and entropy change ($\Delta S°$) were calculated to demonstrate that the adsorption of lead(II) ions onto natural adsorbent was endothermic and spontaneous.

Keywords Sand leek · *Allium scorodoprasum L.* · Biomass · Lead · Biosorption · Wastewater treatment

1 Introduction

Heavy metals are a recognized class of environmental pollutants that have adverse impacts on ecosystems. The enhancement in industrial activity and the growth of the human population have both significantly contributed to the widespread occurrence of heavy metals in the environment. Lead is a heavy metal that is of notable concern within this particular group, as it has been identified by the Environmental Protection Agency (EPA) as one of the 129 contaminants that have significant importance. The issue of heavy metal contamination emerges from various human activities, including mining operations, industrial processes, and inadequate waste management practices. These activities result in the emission of heavy metals into the surroundings, resulting in their subsequent accumulation within diverse ecosystems. After being released, heavy metals such as lead(II) ions can last for long durations, hence presenting substantial hazards to both the environment and human well-being. The toxicity of these substances can lead to several detrimental consequences, such as harm to essential bodily organs, interference with biochemical processes, and the potential emergence of serious illnesses [1]. Therefore, it is crucial to understand the causes, and effects of heavy metal contamination to gauge the problem's severity and design effective remediation strategies.

One of the current methods of removal for heavy metals of lead is chemical precipitation [2]. In this method, chemicals such as lime (calcium hydroxide) or sodium hydroxide are added to the contaminated water to raise the pH and induce the precipitation of lead as insoluble lead hydroxide or lead carbonate. These precipitates can then be separated from the water through sedimentation or filtration. However, chemical precipitation has certain limitations as it requires the addition of large amounts of chemicals, which can be costly, and may introduce additional chemical waste. Moreover, the process is pH-dependent, and maintaining the optimal pH range can be challenging in practice. Additionally, the resulting precipitates may not have a high degree of stability, and there is a possibility of re-dissolution under certain conditions, leading to incomplete removal of lead.

✉ Hasan Arslanoğlu
hasan.arslanoglu@comu.edu.tr

[1] Faculty of Health Sciences, Department of Nutrition and Diet, Sivas Cumhuriyet University, 58140 Sivas, Turkey

[2] Engineering Faculty, Chemical Engineering, Çanakkale Onsekiz Mart University, Çanakkale, Turkey

Adsorption onto activated carbon is a different technique. This extremely porous material has a huge surface area and offers several adsorption sites for the binding of lead(II) ions. The activated carbon is typically used in a fixed-bed column or as a powdered form added directly to the water. The lead(II) ions are attracted to the surface of the carbon through Van der Waals forces or other chemical interactions, effectively removing them from the water [3]. Despite its efficiency in removing heavy metals, conventional activated carbon may have limitations in terms of cost and sustainability. It is typically derived from non-renewable sources such as coal or petroleum, and its production involves energy-intensive processes. Compared to these methods, activated carbon derived from algae offers advantages such as sustainability, cost-effectiveness, high adsorption capacity, selectivity, and faster removal kinetics, making it a viable substitute for heavy metal (lead) removal [4, 5]. Therefore, there is a need to explore alternative approaches for the effective and sustainable removal of lead(II) ions from contaminated water.

Turkey has an important position in the world in terms of plant population diversity. There are approximately 300–315,000 plant species in the world, and 85–90% of them are flowering plants. There are approximately 10,000 cultivated and naturally growing plant species in our country, and more than 1000 of these plant species are used as medicinal and aromatic plants. Medicinal and aromatic plants are used in many areas such as pharmaceuticals, food, cosmetics, insecticides, and medical [6].

Allium scorodoprasum L. subsp. rotundum (L.) Stearn (*Allium rotundum L.*) is a medicinal and aromatic plant that belongs to the Alliaceae family and grows naturally in many countries of the world, including our country. *Allium rotundum* L., a perennial bulbous plant, belongs to the *Allium* genus. The genus Allium is the largest and most characteristic member of the Alliaceae family, which includes more than 800 species, 15 subgenera, and 72 sections [7]. Members of this genus have been consumed since ancient times due to their flavor and aroma compounds. Most types are widely used in folk medicine [8]. The genus *Allium* L. (Alliaceae) exhibits a variety of species with different morphological characteristics in terms of ecological habitats and especially life forms (bulb and rhizome). Most species of this genus are used as vegetables, herbal medicine, and decorative ornamental plants with economic value. These plants are generally bulbous and perennial [9]. It has a wide distribution in the world, especially in the northern hemisphere. *Allium rotundum* (L.) is from the same family as onion, garlic, and leek, known as *allium* vegetables, and is used as food in many regions of Turkey. *Allium* vegetables are some of the oldest cultivated plants in the world. Today, it is known that there are many plants belonging to the *Allium* family growing in Europe, North America, North Africa, and Asia, and each of them has different shapes, tastes, and colors. Many of these plants are used as vegetables, spices, and medicine. Many of them are widely consumed due to their high nutritional properties and aromatic properties [10, 11]. *Allium* vegetables are rich in thiosulfate and organosulfur compounds that play an important role in cell biochemistry. Organosulfur compounds are present in many foods and are used to add flavor to foods. *Allium* vegetables are used in folk medicine in Egypt, China, and India due to the antibiotic, antiseptic, and antithrombotic properties of their organosulfur compounds. These vegetables have protective properties against many diseases such as cancer, obesity, cardiovascular diseases, diabetes, hypercholesterolemia, and hypertension [12].

Allium rotundum L., which has medicinal properties, is widely known in the world as wild leek [13]. It is known among the public by names such as wild garlic, dice garlic, deli leek, korma, coalen, it onion, silim onion, kurat, sirmo, and cracklangus. It is known as stone garlic in the Hatay region, as wild onion in Afyonkarahisar, as emirem in Konya/Beyşehir Kurucaova Town, and as crazy leek in Aksaray, and many other provinces. Both the bulbs and fresh leaves of the plant are eaten raw or cooked in different ways and are used as spices in dishes. In addition to having an important place in folk medicine due to the healthy effects of the plant, it is preferred as a flavor element of many foods, especially Van herb cheese, because it is an aromatic plant. This plant grows naturally in many provinces of our country [14].

There is almost no scientific data in the literature about *Allium rotundum* L., which is an alternative plant consumed for its healthy effects as well as being used as food by the public. For this reason, it is very important to scientifically elucidate the health effects of such plants, which are widely used in folk medicine. In this study, sand leek (*Allium scorodoprasum* L.), a natural biomass, was prepared, and its adsorbent properties were investigated for the removal of lead ions from aqueous media. This natural adsorbent was characterized by FT-IR, SEM–EDX, and PZC analyses. The adsorbent properties of the Ch-V composite for Pb^{2+} were evaluated in terms of pH, concentration, kinetics (time), thermodynamics (temperature), and recovery of adsorption.

2 Material and method

2.1 Chemicals and reagents

$Pb(NO)_3$, KNO_3, HCl, HNO_3, NaOH, C_2H_5OH, and all other chemicals used in this study were of analytical purity (Sigma Aldrich). Pb^{2+} ion stock solutions were prepared by dissolving the appropriate amount of $Pb(NO)_3$ in deionized water.

2.2 Instrumentation

The functional groups on the *Allium scorodoprasum* L. biosorbent before/after Pb^{2+} ions biosorption were determined using the FT-IR (ATR, Bruker Model: Tensor II) technique. The changes in surface morphology of the *Allium scorodoprasum* L. biosorbent before/after Pb^{2+} ions biosorption, along with the identification of different elements, were analyzed by SEM–EDX (TESCAN MIRA3 XMU). The Pb^{2+} ion concentrations were determined using the PAR method with a UV–Vis spectrophotometer (UV-DR-6000; Shimadzu, China) at $\lambda = 519$ nm [15, 16].

2.3 Biosorbent collection and preparation

Fresh *Allium scorodoprasum* L. samples used in this study were collected from the Zara district of Sivas, Turkey. Then, the samples were washed several times with deionized water and dried at 25 °C. Dried *Allium scorodoprasum* L. samples were ground and stored in a polystyrene container for use in biosorption studies.

2.4 Biosorption procedure

Pb^{2+} ion removal with *Allium scorodoprasum* L. biosorbent was investigated using the batch biosorption method. The main factors examined are pH, contact time, adsorbent dosage, temperature, and initial Pb^{2+} concentration. In each experimental set, a fixed dosage of 100 mg of biosorbent was added to 10-mL solutions consisting of 1000 mg L^{-1} Pb^{2+} with stirring for 24 h at room temperature. Then, the solid and liquid phases were separated, and the supernatant concentration and maximum absorbance of Pb^{2+} ions were measured using a UV–Vis spectrophotometer. Biosorption%, Q (mol kg^{-1}) and Recovery% were calculated using Eq. 1–3:

$$Biosorption\% = \left[\frac{C_i - C_f}{C_i}\right] \times 100 \quad (1)$$

$$Q = \left[\frac{C_i - C_f}{m}\right] \times V \quad (2)$$

$$Recovery\% = \frac{Q_{des}}{Q_{ads}} \times 100 \quad (3)$$

where C_i, C_f, m, V, and Q represent the amount of adsorbed (mg g^{-1}), initial, and equilibrium liquid-phase concentrations of the Pb^{2+} ion (mg L^{-1}), the adsorbent mass (mg), and the volume of the solution (L), respectively.

3 Results and discussion

Available literature has highlighted the potential of *Allium scorodoprasum* L. as an adsorbent material, with its positive adsorption capabilities demonstrated in various studies. *Allium scorodoprasum* L. offers several advantages, including its abundant availability, low cost, and environmental friendliness. Herein, the applications for *Allium scorodoprasum* L. have been explored and optimized to enhance its adsorption properties. The optimization of different parameters such as pH, contact time, initial lead(II) ion concentration, adsorbent dosage, and temperature has been conducted to determine the optimal conditions for efficient lead(II) ion removal. The adsorption process followed the Langmuir isotherm model, suggesting a favorable adsorption behavior. The mechanisms of lead(II) ion adsorption onto *Allium scorodoprasum* L. involve surface complexation, ion exchange, and electrostatic interactions. The presence of functional groups on *Allium scorodoprasum* L., which are carboxyl, hydroxyl, and amine groups, plays a potential role in the adsorption process. The understanding of these mechanisms can aid in the design and optimization of *Allium scorodoprasum* L.-based adsorption systems. In this study, applications for *Allium scorodoprasum* L. have been explored and optimized to enhance its adsorption properties. These findings were further verified by doing a kinetic analysis.

3.1 FT-IR and SEM–EDX analyses

FT-IR spectra were taken to identify the functional groups of *Allium scorodoprasum* L. and Pb^{2+} ion biosorbed *Allium scorodoprasum* L. Figure 1 shows the functional groups of *Allium scorodoprasum* L. and Pb^{2+} biosorbed *Allium scorodoprasum* L. As noted by Şenol Arslan 2023, *Allium*

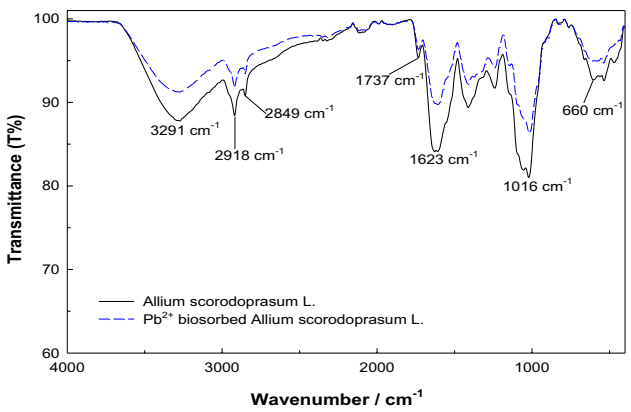


Fig. 1 FT-IR spectra of *Allium scorodoprasum* L. (a) $Pb.^{2+}$ biosorbed *Allium scorodoprasum* L. (b)

scorodoprasum L. biomass exhibited similar spectral patterns. It showed a strong band corresponding to OH stretching vibrations in the range of 3291 cm^{-1}; NH_2 stretching vibrations were observed at 2918 cm^{-1} and 2849 cm^{-1}. The peak at 1732 cm^{-1} is attributed to C = O stretching vibrations, the peak at 1623 cm^{-1} is attributed to C = C stretching vibrations, the peak at 1016 cm^{-1} is attributed to S = O stretching vibrations, and the peak at 660 cm^{-1} is attributed to C–S stretching vibrations [17].

When the FT-IR spectrum of *Allium scorodoprasum* L. was examined after Pb^{2+} biosorption, increases and decreases in the intensities of the characteristic absorption peaks were determined. These changes observed before and after biosorption can be attributed to electrostatic interactions and surface complexation reactions between functional groups and Pb^{2+} ions [1].

SEM images of *Allium scorodoprasum* L. biosorbent before and after Pb^{2+} ion biosorption are given in Fig. 2. It was observed that the surface morphology of *Allium scorodoprasum* L. biosorbent (Fig. 2a) was different from the biosorbent Pb^{2+} ions (Fig. 2b). It was seen that the surface of the *Allium scorodoprasum* L. biosorbent became smoother after the biosorption of Pb^{2+} ions.

As shown in Fig. 2c, d, the EDX analysis results showed that there were increases and decreases in the inorganic components after the biosorption of Pb^{2+} ions, indicating changes in weight percentage. In light of this information, it was thought that more than one mechanism, such as surface complexation and electrostatic interactions, played a role in the biosorption of Pb^{2+} ion onto *Allium scorodoprasum* L. biosorbent.

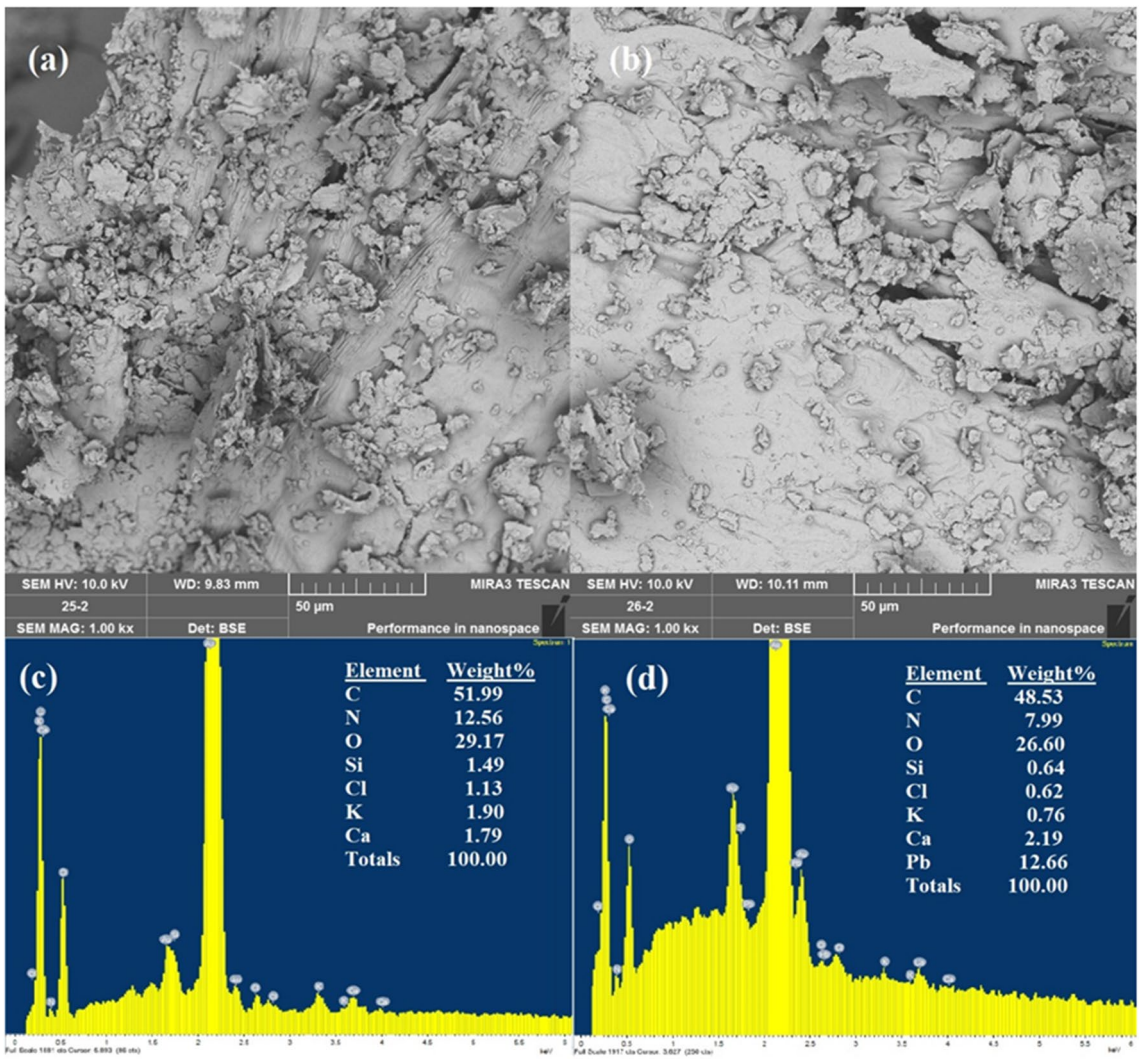


Fig. 2 SEM images of *Allium scorodoprasum* L. (**a**, **c**) $Pb.^{2+}$ biosorbed *Allium scorodoprasum L.* (**b**, **d**)

3.2 Effect of pH on biosorption and pHpzc for *Allium scorodoprasum* L.

The pH value of the biosorption medium is one of the important parameters controlling the biosorption process. In biosorption processes from liquid phase to solid phase, the ionic character of the adsorbate to be removed from the environment and the surface functional groups of the biosorbent are significantly affected by the pH value of the environment. Especially in the biosorption of metals from aqueous solution, the change in the pH value of the solution can cause effects such as hydrolysis, precipitation, redox reactions, and formation of complex compounds in the metal ions in the environment.

To examine the effect of pH on Pb^{2+} ion biosorption to *Allium scorodoprasum* L. biosorbent, pH was studied in the range of 1.0–5.5 (Fig. 3). When Fig. 3 was examined, it was seen that the removal of Pb^{2+} ions increased with increasing solution pH. This increase in biosorption capacity with increasing pH value can be explained by the decrease in the concentration of H^+ ions in an alkaline medium. At low pH values, the biosorption medium is acidic and contains more H^+ ions than the alkaline medium. Since the H^+ ions in the medium will be attracted to the active centers on the biosorbent surface, they create a competing ion effect for Pb^{2+} ions, causing the biosorbent surface to be positively charged. In this case, the electrostatic attraction between the positively charged Pb^{2+} ions in the medium and the positively charged biosorbent surface decreases. It was observed that biosorption efficiency was at maximum at pH 4.5. Pb^{2+} removal was found to be 89% at pH 4.5. After pH 4.5, it was observed that the biosorption efficiency started to decrease. When pH > 5.5, Pb^{2+} ions in the solution environment tend to precipitate in the form of hydroxyls. Since there tend to be more Pb^{2+} ions at pH values < 5.5, the optimum pH value for biosorption experiments is recommended in this study as pH 4.5, which is the natural solution of 1000 mg L^{-1} Pb^{2+} ions:

$$Pb^{2+}_{(aq)} + OH^{-}_{(aq)} \rightarrow Pb(OH)_{2(k)} \quad (4)$$

The surface charge of *Allium scorodoprasum* L. biosorbent was found using the solid addition method [18]. Measurements were carried out at room temperature. ΔpH–pH graph is presented in Fig. 2. The pHpzc value of *Allium scorodoprasum* L. biosorbent was determined as 5.58. At pH < pHpzc values, the biosorbent surface will be positive, which will prevent positively charged Pb^{2+} ions from approaching the biosorbent surface. Because H^+ ions compete with Pb^{2+} ions, the interaction of Pb^{2+} ions with the biosorbent surface may decrease. This explains the low biosorption efficiency at low pH values. With increasing pH, pH > pHpzc will occur, and the biosorbent surface becomes negative. Electrostatic interactions occur between the negative biosorbent surface and Pb^{2+} ions, which increases the biosorption efficiency.

3.3 Biosorbent dose effect

The effect of the biosorbent dose on the biomass of *Allium scorodoprasum* L. was performed by changing the biosorbent dose between 1 and 20 g L^{-1} and balancing it with 1000 mg L^{-1} and 10 mL Pb^{2+} solutions. Figure 4 shows the effect of biosorbent dosage on Pb^{2+} ion removal efficiency. By increasing the biomass dosage from 1 to 20 g L^{-1}, the removal efficiency increases from 20 to 97%. This is because increasing the biosorbent dosage gradually increases the active biosorption areas for Pb^{2+} ions. It was observed that there was a slow change in biosorption efficiency after

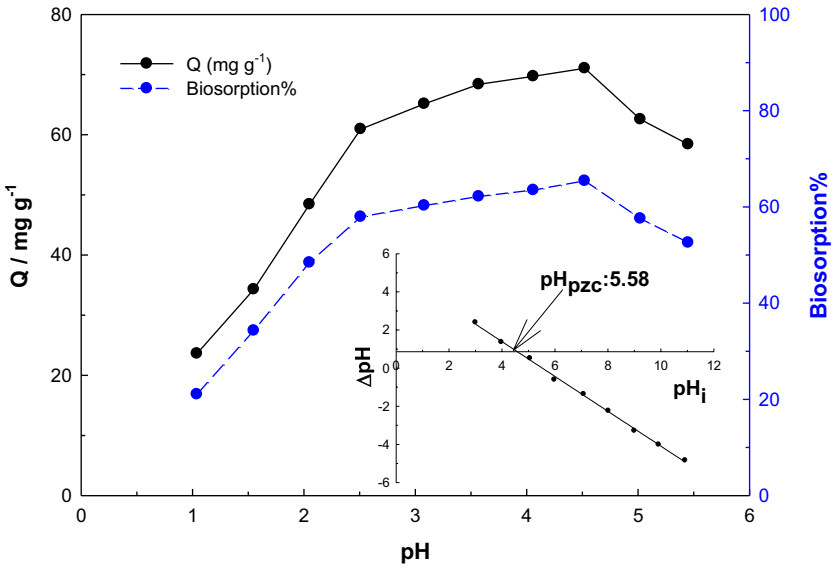


Fig. 3 Effect of pH on biosorption ($[Pb^{2+}]_0$: 1000 mg L^{-1}, amount of biosorbent: 10 g L^{-1}, pH 1.0–5.5, contact time:24 h, temperature: 25 °C), and pHpzc for *Allium scorodoprasum* L

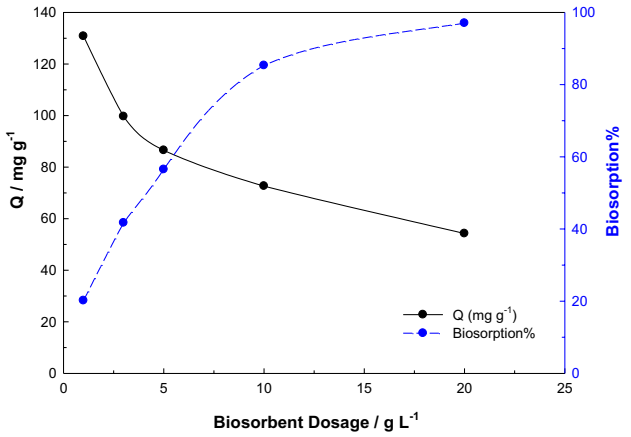


Fig. 4 Effect of adsorbent dose on biosorption ($[Pb^{2+}]_0$, 1000 mg L^{-1}; biosorbent dose, 1, 3, 5, 10, and 20 g $L.^{-1}$; natural pH, 4.5; contact time, 24 h; temperature, 25 °C)

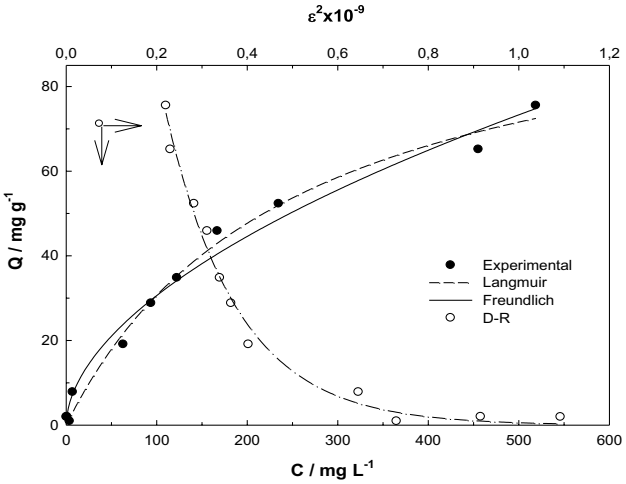


Fig. 5 Biosorption isotherms ($[Pb^{2+}]_0$, 50–1000 mg L^{-1}; biosorbent dose, 10 g $L.^{-1}$; natural pH, 4.5; contact time, 24 h; temperature, 25 °C)

the biosorbent dose was 10 g L^{-1}. Further increasing the amount of biosorbent does not cause a significant increase in biosorption since the Pb^{2+} concentration is constant. For these reasons, a dose of 10 g L^{-1} biosorbent was used in Pb^{2+} ion biosorption experiments on *Allium scorodoprasum* L. biosorbent.

3.4 Biosorption isotherms

Adsorption isotherms define the relationship between the amount adsorbed per unit mass of adsorbate at constant temperature and the adsorbate concentration. Langmuir and Freundlich models are popular two-parameter models that are widely used to describe adsorption isotherms.

The Langmuir model is widely used in solid–liquid systems. This model assumes that the adsorbate surface is homogeneous and of equal energy and that the adsorbate is adsorbed as a monolayer [19]. It assumes that all sites on the adsorbate surface have the same probability of being occupied. The Freundlich isotherm describes the multilayer adsorption process on heterogeneous surfaces. The model assumes that bond strength decreases as the occupancy of active adsorptive sites increases [20]. The Dubinin-Radushkevich (D-R) model also evaluates the adsorption process energetically, assuming that adsorption is related to surface porosity and pore volume [21].

To explain the biosorption mechanism, it is necessary to determine the biosorption isotherm model that is most compatible with experimental data. The fit graphs for Langmuir, Freundlich, and D-R isotherm models in the biosorption process of Pb^{2+} ions to *Allium scorodoprasum* L. biosorbent are presented in Fig. 5, and the parameters derived from these models are presented in Table 1. When Fig. 5 is examined, it is seen that the initial biosorption efficiency increases with increasing concentration. When there is an excess of Pb^{2+} ions in the biosorption medium, the active centers on the biosorbent surface are rapidly covered by the ions in the medium, and the biosorption process, which progresses more slowly over time, reaches equilibrium.

Looking at the R^2 values given in Table 1 for the Langmuir and Freundlich models, it was seen that the isotherm most compatible with the experimental data was the Freundlich model. Accordingly, the biosorption process of Pb^{2+} ions onto *Allium scorodoprasum* L. biosorbent can be defined as monomolecular adhesion on heterogeneous surfaces. In different studies on Pb^{2+} ion removal, processes that can be explained by both adsorption models, similar to the one in this study, were determined (Table 2). X_F, which is a measure of adsorption capacity from the Freundlich model, was found to be 2.52, and β surface heterogeneity was found

Table 1 Parameters calculated from Langmuir, Freundlich, and D-R isotherm models

Isotherm model	Parameter	Value
Langmuir	Q_L (mg g^{-1})	107
$Q = \frac{Q_L C_e}{1+K_L C_e}$	K_L (L mg^{-1})	0.00401
	R^2	0.990
Freundlich	X_F	2.52
$Q = X_F C_e^{\beta}$	β	0.543
	R^2	0.985
D-R	X_{DR} (mg g^{-1})	294
$Q = X_{DR} e^{-(K_{DR}\varepsilon^2)}$		
$\varepsilon = RTln\left(1+\frac{1}{C_e}\right)$	$-K_{DR} \times 10^9$/mol^2 KJ^{-2}	6.28
$E_{DR} = (2K_{DR})^{-0.5}$	E_{DR}/kJ mol^{-1}	6.34
	R^2	0.989

Table 2 Isotherm modeling on the biosorption of Pb^{2+} ions onto another adsorbent in literature

Adsorbent	pH	mg/g from Langmuir model	Reference
Polymethoxyethyl acrylamide		81.02	[22]
Tobacco leaves		39.60	[23]
Hazelnut shells		28.18	[24]
Chitosan-diatomite composite	4.0	31.91	[25]
Cane bagasse		7.29	[26]
Olive tree residues treated with nitric acid		116	[27]
Chitosan and activated charcoal		125	[28]
Bamboo-based activated charcoal		142	[29]
Magnetic magnetite		53.11	[30]
Rhizopus arrhizus	4.5	2.643	[31]
Powder activated carbon	-	20.07	[32]
Crab shell and arca shell	5.5	19.83 and 18.33	[33]
Bacillus sp.	3.0	92.27	[34]
Caulerpa lentillifera (Green macroalga)	5.0	28.7	[35]
Chaff	5.5	12.4	[36]
Gelidium algae	5.0	64	[37]
Chitosan-dolomite composite beads	4.0	67.01	[38]
Mango peel		99.05	[24]
lichen (*Evernia prunastri*)	4.0	13.88	[39]
Allium scorodoprasum L. biomass	4.5	107	This study

to be 0.543. The fact that the β value found from the Freundlich model was less than 1 showed that the biosorption process of Pb^{2+} ions into the *Allium scorodoprasum* L. biosorbent was favorable under the studied conditions. From the Langmuir isotherm model, the maximum biosorption capacity was found to be 107 mg g^{-1}, and the K_L value was 0.00401 L mg^{-1}.

A comparison of the maximum biosorption capacity of Pb^{2+} ions to various sorbents reported in the literature, and *Allium scorodoprasum* L. biosorbent is presented in Table 2. From this table, it can be seen that the maximum sorption capacity of *Allium scorodoprasum* L. biosorbent is higher than that of most adsorbents. This supported that *Allium scorodoprasum* L. biosorbent can be recommended as a potential alternative biosorbent in the removal of Pb^{2+} ions from wastewater.

The biosorption energy derived from fitting the experimental data to the D-R model was found to be 6.34 kJ mol^{-1}. If the biosorption energy is $8 < E < 16$ kJ mol^{-1}, it indicates that the biosorption process is proceeding chemically, and if $E < 8$ kJ mol^{-1}, it indicates that the biosorption process is proceeding physically [40]. In this case, it means that the biosorption process of Pb^{2+} ions into the biosorbent of *Allium scorodoprasum* L. is physical.

3.5 Biosorption kinetics

Biosorption kinetics describes the solute retention that controls the residence time of the biosorbent at the solid–liquid interface, providing information about the reaction pathways and mechanism of the biosorption reaction. Kinetic parameters, which are very important in the design of biosorption systems, are used to explain the biosorption rate and the steps effective in the biosorption mechanism. To explain the biosorption process of Pb^{2+} ions on *Allium scorodoprasum* L. biosorbent, Lagergren's pseudo-first-order (PFO) [41], pseudo-second-order (PSO) kinetics [42], and intraparticle diffusion (IPD) [43] models were used.

Fitting graphs of PFO, PSO, and IPD kinetic models in the biosorption process of Pb^{2+} ions to *Allium scorodoprasum* L. biosorbent (Fig. 6), and the parameters derived from these models are presented in Table 3. When the curves in Fig. 6 were examined, it was seen that biosorption occurred rapidly during the first 180 min, and biosorption slowed down, and equilibrium was reached in 240 min. Since there was an excess of Pb^{2+} ions in the biosorption medium at the beginning, the biosorbent surface was quickly covered by the Pb^{2+} ions in the medium, and over time, the slower biosorption process reached equilibrium. The optimum biosorption time was determined as 240 min.

When the correlation coefficients (R^2) of the PFO, and PSO models presented in Table 3 were examined, it was understood that the Pb^{2+} biosorption mechanism performed at pH 4.5 and 298 K temperature was compatible with the PFO model. In addition, it was seen that the biosorption capacity values calculated from the model equation and the experimentally determined values were

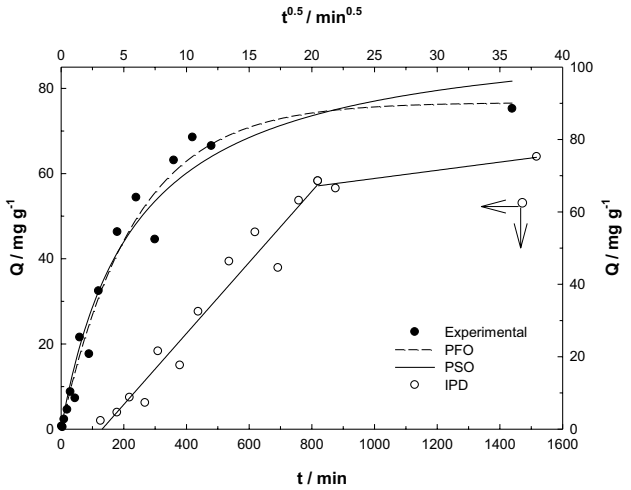


Fig. 6 Biosorption kinetics $(Pb^{2+}]_0$, 1000 mg L^{-1}; biosorbent dose, 10 g $L.^{-1}$; natural pH, 4.5; contact time, 2–1440 min; temperature, 25 °C)

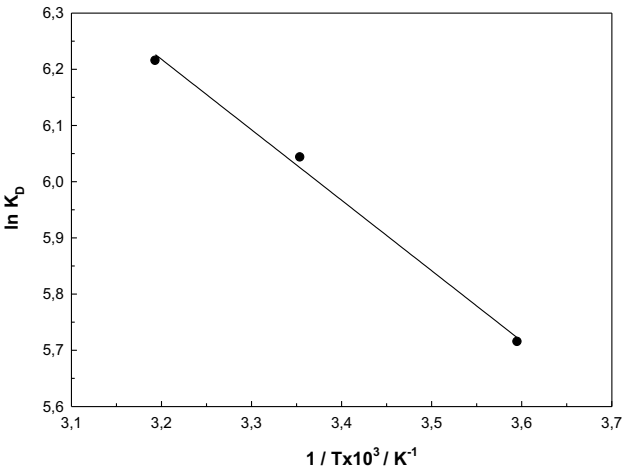


Fig. 7 Biosorption thermodynamics ($[Pb^{2+}]_0$, 1000 mg L^{-1}; biosorbent dose, 10 g $L.^{-1}$; natural pH, 4.5; contact time, 24 h; temperature, 5 °C, 25 °C, and 40 °C)

Table 3 The calculated parameters from PFO, PSO, and IPD kinetic models

Kinetic model	Parameter	Value
PFO	Q_t/mg g^{-1}	75.2
$Q_t = Q_e\left[1 - e^{-k_1 t}\right]$	Q_e/mg g^{-1}	76.7
$H_1 = k_1 Q_e$	$k_1 \times 10^3$/min^{-1}	4.29
	$H_1 \times 10^3$/mg g^{-1} min^{-1}	329
	R^2	0.972
PSO	Q_t/mg g^{-1}	75.2
$Q_t = \frac{t}{\left[\frac{1}{k_2 Q_e^2}\right] + \left[\frac{t}{Q_e}\right]}$	Q_e/mg g^{-1}	94.8
	$k_2 \times 10^3$/mg^{-1} g min^{-1} $H_2 \times 10^3$/ mg g^{-1} min^{-1}	0.0456 410
$H_2 = k_2 Q_e^2$	R^2	0.961
IPD	$k_i \times 10^3$/mg g^{-1} $min^{-0.5}$	5790
$Q_t = k_i t^{0.5}$	R^2	0.915

close to each other. In this case, it can be said that the rate-determining step in the biosorption process carried out in this study will be biosorption through physical interactions.

Compatibility of experimental data of biosorption kinetics with the IPD model is presented in Fig. 6. The IPD model, which includes multiple linear curves, predicts several mechanisms [1]. These are (i) transfer of Pb^{2+} ions from the majority of the solution to the liquid film surrounding the biosorbent, (ii) transport of Pb^{2+} ions from the liquid film surrounding the biosorbent (film diffusion), (iii) biosorption of Pb^{2+} ions to the surface of the biosorbent (biosorption), and (iv) diffusion of Pb^{2+} ions into the pores of the biosorbent (intra-particle diffusion). In general, it can be said that

Table 4 Thermodynamic parameters

Temperature/°C	$\Delta H°$/kJ mol^{-1}	$\Delta G°$/kJ mol^{-1}	$\Delta S°$/ $Jmol^{-1}$ K^{-1}	R^2
5	10.4	−13.3	85	0.996
25		−14.9		
40		−16.2		

the biosorption mechanism is a multi-step process consisting of these sequential steps.

3.6 Biosorption thermodynamics

The effect of temperature on Pb^{2+} biosorption was investigated at three different temperatures: 5 °C, 25 °C, and 40 °C, and the results are presented in Fig. 7. An increase in Pb^{2+} biosorption was observed with increasing temperature of the biosorption medium. The increase in biosorption with increasing temperature indicates the endothermic nature of the biosorption process. The increase in biosorption efficiency with temperature can be attributed to the decrease in mass transfer resistance due to the decrease in the boundary layer thickness surrounding the biosorbent [2]. The thermodynamic parameters for Pb^{2+} ion biosorption onto the biosorbent, enthalpy change ($\Delta H°$), entropy change ($\Delta S°$), and Gibbs-free energy change ($\Delta G°$) were calculated using Eqs. 5–8 given below. The parameters derived using these equations are presented in Table 4:

$$K_d = \frac{Q}{C_e} \tag{5}$$

$$\Delta G^{\circ} = -RTln\left(K_d\right) \tag{6}$$

$$lnK_D = \frac{\Delta S^{\circ}}{R} - \frac{\Delta H^{\circ}}{RT} \tag{7}$$

$$\Delta G^{o} = \Delta H^{o} - T\Delta S^{o} \tag{8}$$

The positive enthalpy value indicated that the biosorption process was endothermic. The positive value of entropy indicated the increase in randomness at the solid-solution interface during the biosorption of Pb^{2+} ions onto the active sites of the biosorbent. The negative Gibbs-free energy change indicated the spontaneous nature of the biosorption process [44–46].

3.7 Recovery

Recovery/desorption is the process of removing biosorbed metal from the biosorbent. Recovery of biosorbent is very important in terms of reducing dependence on continuous biomass supply, keeping process costs low, and ensuring the recovery of metal ions adhering to the solid phase. The commonly used practical method for the desorption of heavy metals from the biosorbent surface is leaching with dilute acids. This is because most metals contain an ion exchange mechanism. Increasing the acidity of the metal biosorbent causes metal ions to separate from the biosorbent surface. Pb^{2+} ion desorption experiments to *Allium scorodoprasum* L. biosorbent were carried out with 100 mg biosorbent in 10-mL 1000 mg L^{-1} Pb^{2+} solution at natural pH: 4.5, 25 °C. Then, the desorption of Pb^{2+} ions was carried out by equilibrating the residue with 10 mL of 0.1 mol L^{-1} each of HCl, HNO_3, and ethyl alcohol separately for 20 min. Biomass was regenerated three times (Fig. 8). No deformation was observed in the biosorbent during biosorption-desorption studies. At the same time, it was observed that the biosorption capacity did not decrease significantly. For this reason, *Allium scorodoprasum* L. biomass can be recycled several times without losing biosorption efficiency, which is very important in biomass selection [44–46].

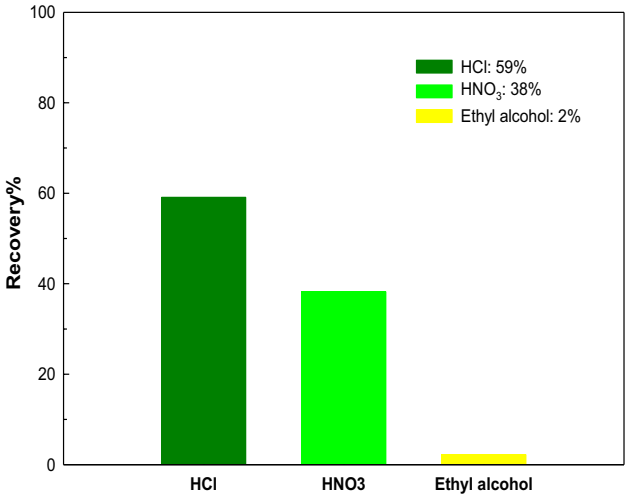


Fig. 8 The effect of recovery on *Allium scorodoprasum* L

4 Conclusion

In this study, batch adsorption experiments were carried out for Pb^{2+} removal from aqueous solution using *Allium scorodoprasum* L. adsorbent. Optimal operating parameters for maximum adsorption, pH of the solution, amount of adsorbent, contact time, and temperature, were selected as pH 4.5, 10 g, 24 h, and 25 ℃. The obtained experimental data were applied to Langmuir, Freundlich, and D-R isotherm models. The monolayer adsorption capacity was found to be 107 mg/g under optimal conditions. The adsorption-free energy calculated from the D-R isotherm was calculated as EDR (6.4 kJ mol^{-1}), which indicates that Pb^{2+} adsorption to *Allium scorodoprasum* L. occurs by the chemical ion exchange mechanism. The negative ΔG° value showed that Pb^{2+} adsorption to *Allium scorodoprasum* L. was possible and spontaneous. A positive ΔH° value depicts the endothermic nature of adsorption.

A positive ΔS° value indicates an increase in the randomness at the adsorbent/solution interface during the adsorption process. By applying experimental data to kinetic models, it was found that Pb^{2+} adsorption onto *Allium scorodoprasum* L. follows pseudo-second-order and intraparticle diffusion rate kinetics. Recovery studies showed that *Allium scorodoprasum* L. composite had good adsorption/desorption performance for Pb^{2+} ions.

Author contribution Zeynep Mine Şenol: analysis of data, revising the manuscript critically for important intellectual content, approval of the version of the manuscript to be published. Hasan Arslanoğlu: writing, acquisition of data, analysis of data, revising the manuscript critically for important intellectual content, approval of the version of the manuscript to be published, review, and editing,

Funding Open access funding provided by the Scientific and Technological Research Council of Türkiye (TÜBİTAK). The present study was partly supported by the Sivas Cumhuriyet University Projects Commission.

Availability of data and materials The data that support the findings of this study are available from the corresponding author, upon reasonable request.

Declarations

Ethics approval Not applicable.

Consent to participate Not applicable.

Consent for publication Not applicable.

Competing interests The authors declare no competing interests.

Open Access This article is licensed under a Creative Commons Attribution 4.0 International License, which permits use, sharing, adaptation, distribution and reproduction in any medium or format, as long as you give appropriate credit to the original author(s) and the source, provide a link to the Creative Commons licence, and indicate if changes were made. The images or other third party material in this article are included in the article's Creative Commons licence, unless indicated otherwise in a credit line to the material. If material is not included in the article's Creative Commons licence and your intended use is not permitted by statutory regulation or exceeds the permitted use, you will need to obtain permission directly from the copyright holder. To view a copy of this licence, visit http://creativecommons.org/licenses/by/4.0/.

References

1. Arslanoğlu E, Eren MŞ, Arslanoğlu H, Çiftçi H (2023) Modification of grape pulp with citric acid for the production of natural ion exchanger resin and removal of Pb (II) and Cd (II) from aqueous solutions: kinetic, thermodynamics, and mechanism. Biomass Convers Biorefinery 13(3):2349–2362
2. Çiftçi H, Çalışkan ÇE, İçtüzer Y, Arslanoğlu H (2023) Application of activated carbon obtained from waste vine shoots for removal of toxic level Cu (II) and Pb (II) in simulated stomach medium. Biomass Convers Biorefinery, pp 1–13. https://doi.org/10.1007/s13399-023-03774-0
3. Li YH, Di Z, Ding J, Wu D, Luan Z, Zhu Y (2005) Adsorption thermodynamic, kinetic and desorption studies of Pb2+ on carbon nanotubes. Water Res 39(4):605–609
4. Li YH, Ding J, Luan Z, Di Z, Zhu Y, Xu C, ... Wei B (2003) Competitive adsorption of Pb2+, Cu2+ and Cd2+ ions from aqueous solutions by multiwalled carbon nanotubes. Carbon 41(14): 2787–2792
5. Elzinga EJ, Rouff AA, Reeder RJ (2006) The long-term fate of Cu2+, Zn2+, and Pb2+ adsorption complexes at the calcite surface: an X-ray absorption spectroscopy study. Geochim Cosmochim Acta 70(11):2715–2725
6. Gürbüz B, Arif İPEK, Ayvaz N (2011) Türkiye florasındaki Origanum türlerinin yayılış alanları ve ticareti. Türk Bilimsel Derlemeler Dergisi 2:5–58
7. Fritsch RM, Blattner FR, Gurushidze M (2010) New classification of Allium L. subg. Melanocrommyum (Webb & Berthel.) Rouy (Alliaceae) based on molecular and morphological characters. Phyton (Horn) 49(2):145–220
8. Mitic VD, Stankov-Jovanovic VP, Ilic MD, Cvetkovic JS, Dimitrijevic MV, Stojanovic GS (2014) *In vitro* antioxidant activity of methanol extract of *Allium scorodoprasum*. Bulg J Agric Sci 20:1130–1136
9. Zouari S, Ketata M, Boudhrioua N, Ammar E (2013) *Allium roseum* L. volatile compounds profile and antioxydant activity for chemotype discrimination-case study of the wild plant of Sfax (Tunisia). Ind Crops Prod 41:172–178
10. Benkeblia N, Lanzotti V (2007) Allium thiosulfinates: chemistry, biological properties and their potential utilization in food preservation. Food 1:193–201
11. Seyrek EŞ, Yalcin E, Yilmaz M, Kök BV, Arslanoğlu H (2020) Effect of activated carbon obtained from vinasse and marc on the rheological and mechanical characteristics of the bitumen binders and hot mix asphalts. Constr Build Mater 240:117921
12. Pardo JE, Escribano J, Gómez R, Alvarruiz A (2007) Physical-chemical and sensory quality evaluation of garlic cultivars. J Food Qual 30:609–622
13. Mehrabi AA, Nasab BF (2012) In-vitro Culture of *Allium scorodoprasum* spp. *rotundum*: Callus induction, somatic embryogenesiis and direct bulblet formation. Int J Agric Crop Sci 4(1):1–7
14. Tasci B, Koca I (2015) Use of *Allium scorodoprasum* L. *subsp. rotundum* (L.) *stearn* as food, 7th International Symposium on Edible Alliaceae, Nigde, Turkey, 21–25 May
15. Şenol ZM (2021) A chitosan-based composite for adsorption of uranyl ions; mechanism, isothems, kinetics and thermodynamics. Int J Biol Macromol 183:1640–1648
16. Türk FN (2023) Removal of basic blue 9 (methylene blue) dyestuff from aqueous solutions using citric acid modified (esterified) sugar beet pulp. Sugar Tech 25(5):251–1261
17. Sezer GG, Yeşilel OZ, Şahin O, Arslanoğlu H, Erucar I (2017) Facile synthesis of 2D Zn (II) coordination polymer and its crystal structure, selective removal of methylene blue and molecular simulations. J Mol Struct 1143:355–361
18. Liang YM, Jun M, Liu W (2007) Enhanced removal of lead (II) and cadmium (II) from water in alum coagulation by ferrate (VI) pretreatment. Water Environ Res 79(12):2420–2426
19. Langmuir I (1918) Adsorption of gases on plane surfaces of glass, mica and platinum. J Am Chem Soc 40:1361–1403
20. Freundlich H (1907) Ueber die Adsorption in Loesungen. Z Phys Chem 57:385–470
21. Dubinin MM, Radushkevich LV (1947) The equation of the characteristic curve of the activated charcoal. Proc Acad Sci Phys Chem Sect USSR 55:331–337
22. Şölener M, TunaliAkar S, Ozcan A, Ozcan A, Gedikbey T (2008) Adsorption characteristics of lead(II) ions onto the clay/poly(methoxyethyl) acrylamide (PMEA) composite from aqueous solutions. Desalination 223:308–322
23. Qi BC, Aldrich C (2008) Biosorption of heavy metals from aqueous solutions with tobacco dust. Bioresour Technol 99:5595–5601
24. Pehlivan E, Altun T, Cetin S, Iqbal Bhanger M (2009) Lead sorption by waste biomass of hazelnut and almond shell. J Hazard Mater 167:1203–1208
25 Şenol ZM, Şimşek S (2020) Removal of Pb2+ ions from aqueous medium by using chitosan-diatomite composite: equilibrium, kinetic and thermodynamic studies. J Turk Chem Soc Sect A: Chem 7(1):307–318
26 Martín-Lara MA, Rico ILR, García GB, de Hoces MC, de la CA, Vicente I (2010) Modification of the sorptive characteristics of sugarcane bagasse for removing lead from aqueous solutions. Desalination 256:58–63
27. Boudrahem F, Aissani-Benissad F, Audonnet F, Vial C (2011) Kinetics and equilibrium adsorption of lead (II) ions on olive residues: effects of chemical activation. Alger J Environ Sci Technol Mon 56:1946
28. Ge H, Fan X (2011) Adsorption of Pb2+ and Cd2+ onto a novel activated carbon-chitosan complex. Chem Eng Technol 34:1745–1752
29. Yang CS, Jang YS, Jeong HK (2014) Bamboo-based activated carbon for supercapacitor applications. Curr Appl Phys 14(12):1616–1620
30. Rajput S, Pittman CU, Mohan D (2016) Magnetic magnetite (Fe3O4) nanoparticle synthesis and applications for lead (Pb2+) and chromium (Cr6+) removal from water. J Colloid Interface Sci 468:334–346
31. Bahadir T, Bakan G, Altas L, Buyukgungor H (2007) The investigation of lead removal by biosorption: an application at

storage battery industry waste waters. Enzyme Microb Technol 41(1–2):98–102
32. Matheickal JT, Yu Q (1996) Biosorption of lead from aqueous solution by macro-fungi Phellinus badius, in: Proceedings of the 10th National Convention of Royal Australian Chemical Institute, Adelaide, Australia
33. Dahiya S, Tripathi RM, Hegde AG (2008) Biosorption of lead and copper from aqueous solutions by pre-treated crab and arca shell biomass. Bioresour Technol 99:179–187
34. Tunali S, Cubak A, Akar T (2006) Removal of lead and copper ions from aqueous solutions by bacterial strain isolated from soil. Chem Eng J 115:203–211
35. Pavasant P, Apiratikul R, Sungkhum V, Suthiparinyanont P, Wattanachira S, Marhaba TF (2006) Biosorption of Cu2+, Cd2+, Pb2+, and Zn2+ using dried marine green macroalga Caulerpa lentillifera. Bioresour Technol 97(18):2321–2329
36. Han R, Zhang W, Zou J, Shi H, Liu Y (2005) Equilibrium biosorption isotherm for lead ion on chaff. J Hazard Mater 125:266–271
37. Vilar VJP, Botelho CMS, Boaventura RAR (2005) Influence of pH, ionic strength and temperature on lead biosorption by Gelidium and agar extraction algal waste. Process Biochem 40:3267–3275
38. Şenol ZM, Şimşek S (2022) Equilibrium, kinetics and thermodynamics of Pb (II) ions from aqueous solution by adsorption onto chitosan-dolomite composite beads. Int J Environ Anal Chem 102(17):4926–4940
39. Şenol ZM, Gül ÜD, Şimşek S (2019) Assessment of Pb2+ removal capacity of lichen (Evernia prunastri): application of adsorption kinetic, isotherm models, and thermodynamics. Environ Sci Pollut Res 26(26):27002–27013
40. Romero-Gonzalez J, Peralta-Videa JR, Rodrıguez E, Ramirez SL, Gardea-Torresdey JL (2005) Determination of thermodynamic parameters of Cr(VI) adsorption from aqueous solution onto Agave lechuguilla biomass. J Chem Thermodyn 37:343–347
41. Lagergren S (1898) Zur theorie der sogenannten adsorption geloster stoffe, Kongliga Svenska Vetenskapsakademiens. Handlingar 24:1–39
42. McKay G, Ho YS (1999) Pseudo-second order model for adsorption processes. Process Biochem 34:451–465. https://doi.org/10.1016/S0032-9592(98)00112-5
43. Weber WJ, Morris JC (1963) Kinetics of adsorption on carbon from solution. J Sanit Eng Div ASCE 89:31–60
44. Şenol ZM, Çetinkaya S, Arslanoglu H (2023) Recycling of Labada (Rumex) biowaste as a value-added biosorbent for rhodamine B (Rd-B) wastewater treatment: biosorption study with experimental design optimisation. Biomass Convers Biorefinery 13(3):2413–2425
45. Arslanoğlu E, Eren MŞ, Arslanoğlu H, Çiftçi H (2021) Fabrication, characterization, and adsorption applications of low-cost hybride activated carbons from peanut shell-vinasse mixtures by one-step pyrolysis. Biomass Convers Biorefin 3:2321–2335
46. Wang Y, Wang X, Wang X, Liu M, Wu Z, Yang L, Xia S, Zhao J (2013) Adsorption of Pb(II) from aqueous solution to Ni-doped bamboo charcoal. J Ind Eng Chem 19:353–359

Publisher's Note Springer Nature remains neutral with regard to jurisdictional claims in published maps and institutional affiliations.